

# Effects of Anisotropic Interactions on the Structure of Animal Groups

Emiliano Cristiani\* Paolo Frasca† Benedetto Piccoli‡

February 6, 2020

## Abstract

This paper proposes an agent-based model which reproduces different structures of animal groups. The shape and structure of the group is the effect of simple interaction rules among individuals: each animal deploys itself depending on the position of a limited number of neighboring group mates. The proposed model is shown to produce clustered formations, as well as lines and V-like formations. The key factors which trigger the onset of different patterns are argued to be the relative strength of attraction and repulsion forces, and most important, the anisotropy in their application.

**Keywords.** Anisotropic interactions, animal groups, coordinated behavior, self-organization, agent-based models.

**MSC.** 92D50, 92B05.

## 1 Introduction

The investigation of the group behavior in animals has greatly interested scientists and researchers in the past, and has received further attention in the last decades, as an issue of complexity and self-organization phenomena. Recently, it has attracted attention not only from biologists and ethologists, but also from physicists, mathematicians, and engineers. This interest has produced a huge bulk of literature, which is well documented and reviewed, for instance, in [24, 39, 14] [6]. Loosely speaking, the basic idea behind these works is that

---

\*CEMSAC, Università di Salerno, Italy and IAC-CNR, Rome, Italy. E-mail: [emiliano.cristiani@gmail.com](mailto:emiliano.cristiani@gmail.com)

†DIIMA, Università di Salerno, Italy and IAC-CNR, Rome, Italy. E-mail: [paolo.frasca@gmail.com](mailto:paolo.frasca@gmail.com)

‡IAC-CNR, Rome, Italy. E-mail: [b.piccoli@iac.cnr.it](mailto:b.piccoli@iac.cnr.it) Mail: IAC-CNR c/o Dipartimento di Matematica dell'Università di Roma Tor Vergata, Via della Ricerca Scientifica, 00133, Rome, Italy

complex collective behavior arises from simple interaction among neighboring animals. On the wave of this interest, and following this idea, the aim of this paper is to investigate a simple model which is able to reproduce rather different patterns and structures at the group level.

Let us briefly introduce the main features of our model and its relationships with the literature: a detailed description is postponed to Section 2. First, our model is *agent-based*, in the sense that each animal is singularly considered, and is *leaderless*, in the sense that all animals act following the same set of rules and their behavior is not imposed by others. These assumptions are widely used in the literature, and accepted as biologically sound for a variety of species: see, among others, [44, 22, 32, 10, 9].

Second, our model is based on purely *cohesion-repulsion* interactions between group mates. Cohesion allows the group to be formed and stay tight, while repulsion allows to avoid collisions between group mates and keeps them well spaced. This kind of interaction has been widely considered in the literature. In the majority of papers, cohesion and repulsion are combined with a mechanism for velocities alignment. Instead, here we keep aside the issue of alignment, which has received a considerable attention in itself [43, 11], and focus on (the superposition of) cohesion and repulsion: on this respect our approach is close to [44, 30].

Third, each animal interacts with a *limited number* of group mates. The idea of having a limited number of neighbors to be considered for interaction is not new. Indeed, already the work [19] considers attraction to *the* nearest neighbor, while later experimental investigations found interaction with two-four individuals in fish [1]. This fact has been included in several models, among others [44, 22, 23, 32], but it has not always been included in other recent models, for instance [17, 10, 25, 9], in favor of a purely metric notion of neighborhood: interaction occurs with all group mates which are closer than a threshold distance apart. Very recently, the former idea has been brought again to attention by [3], where the authors present experimental results, regarding fairly large flocks of starlings, which imply that interaction occurs with up to six-seven neighbors, no matter how far they are. The same paper also gives some simulation results, which suggest that a better cohesion of the flock can be guaranteed in that way. We also want to point out in the literature a third approach to neighborhood definition, based on Voronoi partitions: its application in biology dates back to [19], and it is well documented in the physicists [16] and engineers [6] literatures.

Fourth, each animal interacts only with group mates which are located around it, in a suitably defined *sensitivity zone*. Restricting the interactions to a sensitivity zone raises the issue of defining its size and shape. On this matter, there is a significant background of works considering limited visual (or sensing) fields: a limitation in the animal's angle of vision has been incorporated in most models, assuming a blind rear zone [22, 23, 10, 20, 29], or distinguishing between front and rear sensitivity [17]. In [25] authors assume repulsion and alignment regions to be elliptical (taking into account body shapes), and cut off these regions by the blind rear area. In the recent paper [31], the authors clearly distinguish between visual field and sensitivity zones, stating that the behav-

ioral rules they use in the model apply only in the front zone. In this paper, we adopt this distinction between sensing and sensitivity limitations. However, up to our knowledge, the anisotropy of sensitivity zones has always been taken just as a given constraint, and not as a potential resource, able to shape the group geometry. Here is the main contribution of our paper: showing that a restricted sensitivity angle can be a key element in determining the structure and shape of an animal group. Indeed we show that changing two parameters, namely two sensitivity angles, for cohesion and repulsion, we obtain more or less elongated cluster formations, and actually *line* formations and *V-like* formations, which are described in Section 3. Note that similar patterns have already been obtained by means of other mathematical models (see for example [16, 17, 31]), the novelty here is that our model is able to reproduce all of them, depending on few parameters. We believe that this can offer new biological insights.

Besides investigating the main issue of the role of anisotropy, we also present some results about the effect of the limiting the number of considered neighbors, and about the influence of the relative strength of cohesion and repulsion on the inter-animal distance: the latter problem relates the results in [30].

The observations drawn from simulations are accompanied by a formal mathematical investigation of the model. In the literature, one can find that a popular approach to the analysis of agent-based flocking models consists in defining a suitable potential function, called “virtual” or “artificial” potential, whose gradient gives the dynamics. This variational approach has been followed by both engineers [41] and biologists [30, 26] (among others) with important results. However, it is not possible to apply it to our model. Indeed, with respect to other models, ours has two main features: *state dependent switching dynamics*, and *asymmetry of interactions*. The former is due to the state dependent definition of the set of group mates which interact with a given animal. This discontinuous state dependence has been included in previous literature: see for instance the treatment in [41], based on non-smooth potentials. The latter feature, instead, is due to the fact that the limited number of interacting neighbors and the restricted sensitivity angles imply that interactions need not to be symmetrical (reciprocal). This fact prevents the application of the virtual potential approach, and indeed it has received little attention in the literature: the paper [37] is a partial attempt in this sense, because it considers a second-order system in which velocity alignment is achieved by asymmetric interactions, but agents’ positions are controlled using symmetrical information exchange. Then, its results are not useful to us, as we are interested in spatial configurations. Overall, we conclude that the mathematical analysis of our model requires a novel approach, which has to include discontinuous and asymmetric interactions among animals.

The rest of the paper is organized as follows. The details about the model are given in Section 2. Then, extensive simulation results are presented in Section 3, whereas Section 4 contains the mathematical analysis. Later, Section 5 discusses the implications of our findings and their biological soundness. We conclude presenting some lines of future research.

## 2 Model definition

The animals in the model are represented by point particles, which have simple continuous-time dynamics. Given  $N \in \mathbb{N}$ , for all  $i \in \{1, \dots, N\}$  and  $t \in \mathbb{R}_{\geq 0}$ , let  $x_i(t) \in \mathbb{R}^2$  represent the position of the  $i$ -th animal, whose evolution is described by the differential equation

$$\dot{x}_i(t) = v_i(x(t)), \quad (1)$$

where  $x(t)$  is the vector  $(x_1(t), \dots, x_N(t))$ . As in [30], animal positions are considered with respect to a coordinate system moving with the group centroid: this means that we are modelling relative movements of the individuals and group structure, rather than its global motion. The velocity  $v_i(x)$  is the sum of two contributions, expressing the tendencies to cohesion and to repulsion,

$$v_i(x) = v_i^c(x) - v_i^r(x).$$

In more detail, each of these contributions depends on the relative position of the other animals,

$$\begin{aligned} v_i^c(x) &= \sum_{j \in \mathcal{C}_i^n} f_c(\|x_j - x_i\|) \frac{x_j - x_i}{\|x_j - x_i\|} \\ v_i^r(x) &= \sum_{j \in \mathcal{R}_i^n} f_r(\|x_j - x_i\|) \frac{x_j - x_i}{\|x_j - x_i\|}. \end{aligned}$$

The following definitions have been used.

- The function  $f_c : \mathbb{R}_{\geq 0} \rightarrow \mathbb{R}_{\geq 0}$  (resp.,  $f_r : \mathbb{R}_{\geq 0} \rightarrow \mathbb{R}_{\geq 0}$ ) describes how each animal is attracted (resp., repelled) by a neighbor at a given distance, assuming  $\|\cdot\|$  denotes the Euclidean norm in  $\mathbb{R}^2$ .
- $\mathcal{C}_i^n$  (resp.,  $\mathcal{R}_i^n$ ) is the set of the (at most)  $n$  animals closest to the  $i$ -th one, which are inside the cohesion (resp., repulsion) sensitivity zone.

The above model is very general, and we need to specialize it by choosing the interaction functions and the shape of the sensitivity zones. We make the following assumptions.

1. The "forces" read  $f_c(s) = F_c s$  and  $f_r(s) = \frac{F_r}{s}$ , where  $F_c$  and  $F_r$  are two positive constants.
2. The sensitivity zones are as depicted in Figure 1. Repulsion acts inside a disk of radius  $R_{sr} > 0$  (*short-range* repulsion) and in an angle  $\alpha_r \in (0^\circ, 360^\circ]$ , whereas cohesion acts in an angle  $\alpha_c \in (0, 360^\circ]$ . Angles are always assumed to be oriented following the horizontal axis, as in the figure. The two angles do not necessarily coincide with the visual/sensitivity field of the animal: they rather represent the zones where cohesion and repulsion are focused.

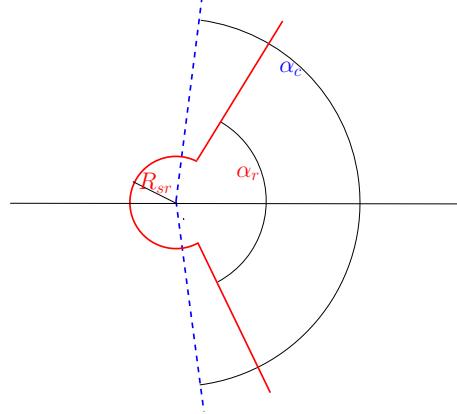


Figure 1: The shape of the sensitivity zones.

3. The speed of each animal  $\|v_i\|$  is bounded from above by a constant  $v_{\max}$ .

The above assumptions result in the system

$$\dot{x}_i(t) = F_c \sum_{j \in \mathcal{C}_i^n} (x_j - x_i) - F_r \sum_{j \in \mathcal{R}_i^n} \frac{(x_j - x_i)}{\|x_j - x_i\|^2}. \quad (2)$$

Some remarks are in order.

- R1. Although the model has dynamics in  $\mathbb{R}^2$ , extension to higher dimensions is straightforward.
- R2. Defining the sets of interacting neighbors of an animal as  $\mathcal{C}_i^n$  and  $\mathcal{R}_i^n$  allows to have an a priori bound on the number of effective neighbors, and then on the sensing and "computational" effort which is required for each animal. This fact, which copes with animals' intrinsic limitations, has been experimentally observed in biology, for fish [1] and birds [3]. The latter paper calls this neighborhood definition *topological*, as opposed to *metric* definitions, based on distance only.
- R3. Our assumption of unbounded sensitivity regions does not intend to imply that animals sensing capabilities extend on an unlimited range, but rather that group dynamics happen in a relatively small area.
- R4. If  $\alpha_c = \alpha_r = 360^\circ$ , the parameter  $R_{sr}$  has no effect, and the interaction is completely isotropic, as in the simulations presented in [3, 7]. Note that, even if there is no preference for any specific direction, the limitation of the number of considered neighbors makes the interactions not reciprocal, i.e. the fact that the  $i$ -th animal interacts with the  $j$ -th does not imply that the  $j$ -th interacts with the  $i$ -th.

R5. By specializing the functions  $f_c$  and  $f_r$ , one can obtain various interaction models. Indeed many proposals can be found in the literature, as reviewed in [44] and [30]. However, the shape of these functions is not the main point in our paper, and thus we have decided to focus on a simple choice, to highlight the innovative part of our approach, i.e. the angle-dependent interactions. Similar considerations are valid also for some features introduced in other models, such as a *neutral zone* around animals [42, 7] or a hierarchical decision tree which allows the repulsion force to have the priority over the cohesion force [17, 7].

### 3 Simulations results

In this section we make use of the agent-based model (2) in order to show the effect of the anisotropic interactions on the shape of the group. Namely, depending on the angles  $\alpha_c$ ,  $\alpha_r$ , and the ratio between repulsive and cohesive forces, we shall obtain either *clusters*, or *lines* or *V-like* formations. These patterns are described in the sequel.

To perform the simulations, it is instrumental the introduction of the constant  $\xi = \sqrt{\frac{F_r}{F_c}}$ , which allows to rewrite (2) as

$$\dot{x}_i(t) = \sum_{j \in \mathcal{C}_i^n} (x_j - x_i) - \xi^2 \sum_{j \in \mathcal{R}_i^n} \frac{(x_j - x_i)}{\|x_j - x_i\|^2}. \quad (3)$$

In equation (3), the unit of length is chosen to be the body length (BL) of the animal, and the time unit (TU) is the inverse of  $F_c$ . Simulations are obtained solving the system of equations (3) via an explicit forward Euler adaptive scheme. Each run starts from a randomly generated initial configuration (contained in square of edge  $L$ ), and ends when the system reaches a steady state. To take into account the uncertainties in sensing and motion of the animals, we include a small uniformly-distributed random disturbance  $\alpha_{\text{noise}}$  on the direction of the velocity. All the system equilibria described in the sequel are robust to such noise. A summary of the parameters and their values is given in Table 1. In the sequel we discuss the role of  $N$ ,  $n$ ,  $\xi$ ,  $\alpha_c$  and  $\alpha_r$ , which are the most significant to us, whereas  $R_{\text{sr}}$ ,  $v_{\text{max}}$ ,  $\alpha_{\text{noise}}$  and  $L$  are kept fixed.

#### 3.1 Clusters

In this paragraph, we describe simulation results when interactions are assumed to be isotropic. These results are not dissimilar from others in the literature (e.g., [30, 26]): we include them for two reasons. First, for comparison with the less usual patterns described in the following paragraphs. Second, because they allow some interesting remarks about the role of the model's parameters  $\xi$  and  $n$ .

Thus, let us assume that  $\alpha_c = \alpha_r = 360^\circ$ . As a consequence, the outcome of the simulations is a cohesive and well spaced cluster. For a better understanding,

Table 1: Model parameters.

Name	Symbol	Unit	Values explored
Forces ratio	$\xi$	BL	0.1–20
Cohesion angle	$\alpha_c$	degrees ( $^\circ$ )	0–360
Repulsion angle	$\alpha_r$	degrees ( $^\circ$ )	0–360
Number of animals	$N$	adimensional	2–200
Number of considered neighbors	$n$	adimensional	1–( $N - 1$ )
Short-range repulsion radius	$R_{sr}$	BL	1
Maximum speed	$v_{\max}$	BL/TU	2–30
Size of initial domain	$L$	BL	15
Noise magnitude	$\alpha_{\text{noise}}$	degrees ( $^\circ$ )	0–10

we make use of an indicator which is largely used in the literature (see for instance [22, 25]): the *mean distance to the nearest neighbor* NND, defined as

$$\text{NND} = \frac{1}{N} \sum_{i=1}^N \min_{j \neq i} \|x_i - x_j\|.$$

We investigate the dependence of NND on the parameter  $\xi$ : simulation results are shown in Figure 2. We observe that NND is an increasing function of  $\xi$ , in

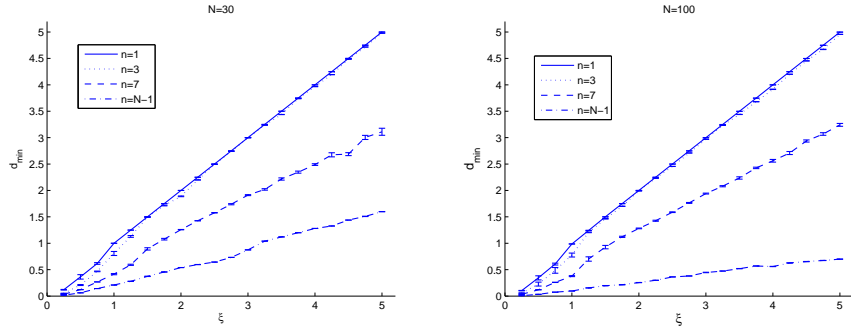


Figure 2: NND as a function of the ratio  $\xi$ , for different values of  $n$ . Error bars denote variance across individuals. Plots assume  $N = 30$  (left) and  $N = 100$  (right).

particular it increases roughly linearly in  $\xi$ . This linear dependence is observed for any choice of  $n$ . Two other features are noticeable: first, if  $n = 1$ , animals asymptotically converge to a *comfortable distance* which is equal to  $\xi$ . Second, for any fixed  $\xi$ , NND decreases as  $n$  increases. Moreover, all these remarks do not depend on  $N$ .

These results can be compared with those in [30]: in that paper, the authors assume that all animals in the group interact among each other, and they

conclude that, the larger the group, the closer packed it is. Our simulations, instead, suggest that the significant parameter is  $n$ , the number of neighbors which is taken into account, rather than  $N$ , the global number of animals. However, from the biological point of view, the number of neighbors  $n$  is not truly a free parameter:  $n$  can not be too large because of the limited sensing and analysis capabilities of the animals, and can not be too small either. For instance, a low value of  $n$  sounds unsafe from the point of view of collision avoidance. Indeed, experimental evidence suggests  $n$  be approximately between 2-3 and 7, depending on species [1, 4].

Figure 2 also shows that the variance of the distance to the nearest neighbor among the animals is quite small. This means that groups are internally uniform, in terms of spacing. This uniformity is also apparent if one looks at the steady-state configurations: three examples are shown in Figure 3. Nevertheless,

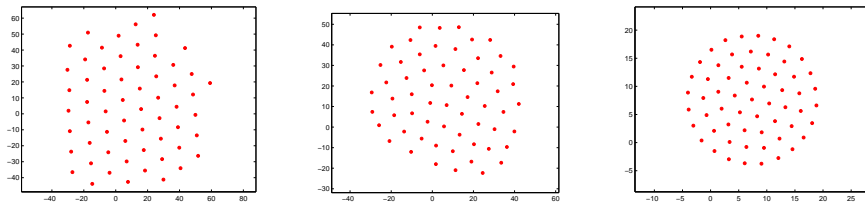


Figure 3: Internal structures of the clusters: from left to right,  $n = 1$  (crystal-like cluster),  $n = 7$  (disordered cluster) and  $n = N - 1$  (circular cluster), obtained with  $\xi = 10$  and  $N = 60$ .

as  $n$  varies, significant modifications are apparent in terms of relative positions. If  $n = 1$ , the animals are deployed to form an hexagonal lattice, reminiscent of a crystal. For intermediate  $n$ 's the internal structure is rather disordered, and if  $n = N - 1$  it is made of concentric circles. Note that crystal-like patterns have also been found in [16] and in [26], where they are compared with the less regular structures obtained in [8].

### 3.2 Lines

In this paragraph we show how restricting the sensitivity field (i.e. reducing  $\alpha_r$  and  $\alpha_c$ ) induces the formation of an elongated group. The key element for the formation of these patterns is a restricted frontal sensitivity field. Let us denote by  $e$  the oriented *elongation* of the group (see for instance [17, 25]), defined as the ratio of the vertical to the horizontal side of the smallest rectangle containing the group, oriented parallel to the direction of the movement. Here we study how  $e$  depends on the angles  $(\alpha_r, \alpha_c)$ , and on  $n$ . Results are summarized in Figure 4, which shows the average and the extreme values of  $e$  over 100 runs as a function of the angles  $(\alpha_r, \alpha_c)$ , for  $n = 1, 7, N - 1$ . It is clear that reducing angles from  $(360^\circ, 360^\circ)$  to  $(40^\circ, 180^\circ)$  affects the elongation of the group. Wide angles (roughly,  $360^\circ > \alpha_r > 200^\circ$  and  $360^\circ > \alpha_c > 270^\circ$ ) induce an average

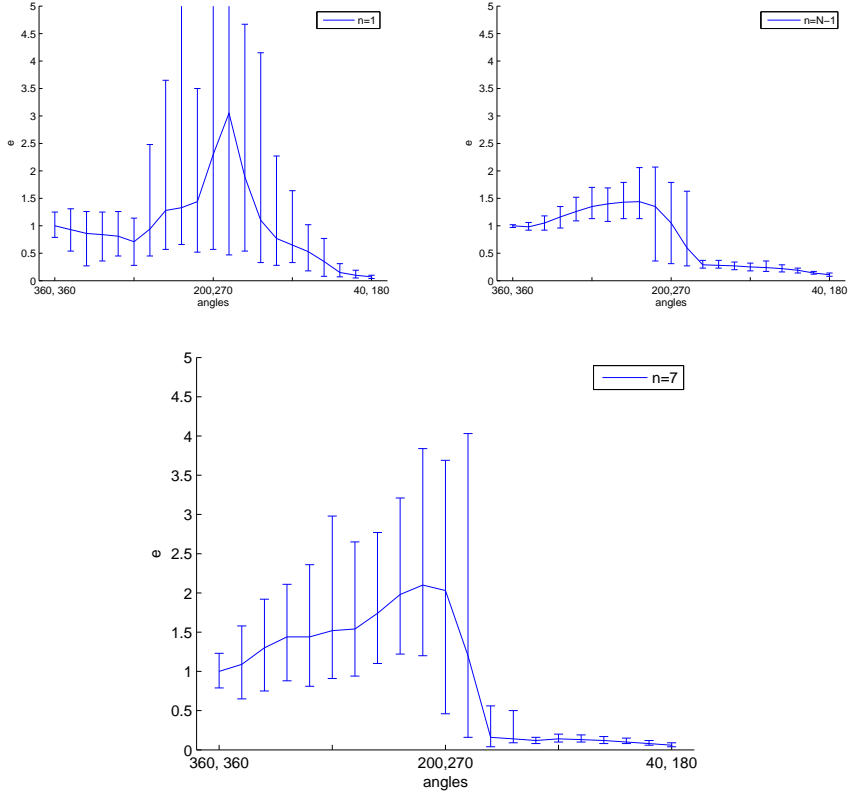


Figure 4: Mean elongation of the group as a function of the sensitivity angles, for  $N = 30$  and different values of  $n$ . The angles are  $(\alpha_r, \alpha_c) = (360^\circ - k16^\circ, 360^\circ - k9^\circ)$ ,  $k = 0, \dots, 20$ . Data come from 100 runs. Error bars are the ranges of the outcomes.

elongation greater than 1, i.e. the group stretches along the vertical direction. Moreover, the range of the outcomes is large, meaning that different initial conditions affect significantly the evolution of the system. In the majority of runs the system does not reach an equilibrium in a reasonable time, and the simulation is stopped after a maximum number of iterations. Conversely, small angles ( $200^\circ > \alpha_r > 40^\circ$  and  $270^\circ > \alpha_c > 180^\circ$ ) lead to small values of  $e$ , with small differences among the runs. In the latter case an equilibrium is always reached, and configuration is strongly elongated along the direction of motion: in the limit case, it is a line. One can also observe a dependence on  $n$ : larger values of  $n$  show a sharper transition to lines than with  $n = 1$ .

To ensure that a stable single-file line sets up, as the one shown in Figure 5, it is instrumental to introduce a slight modification of the general model, cutting-off to zero the repulsion forces which are below a small threshold. This correction

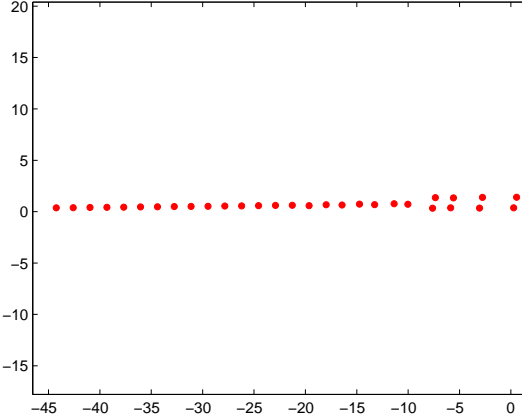


Figure 5: A line formation, obtained with  $\alpha_r = 40^\circ$ ,  $\alpha_c = 180^\circ$ ,  $n = 7$ ,  $\xi = 10$ ,  $N = 30$ . See text for the explanation of the irregularities in the head of the line.

can be understood as a rule of thumb to stabilize the line formation, which is otherwise known to be ill-behaved from the point of view of stability. The latter phenomenon is sometimes called *string instability* in the engineering literature: control theorists interested in controlling lines of vehicles [40, 36] have observed that perturbations propagate down the line in cascade, leading to instabilities. Finally, we note that in Figure 5 some "border effects" are visible in the head of the line (right side): since in this case we chose  $n = 7$ , the animals in the front can not interact with a sufficient number of group mates and then they do not stabilize in a single-file line.

### 3.3 Vees

In this paragraph we show that a restricted frontal *repulsion* range ( $\alpha_r < 180^\circ$ ) induces the formation of V-like patterns. V-like formations have been recently obtained in the literature [31], using an *ad hoc* model motivated by aerodynamics considerations: in our model, instead, V-like formations arise in a wider analysis of the anisotropy effects. Following [21], we adopt a broad definition of V-like formations, which includes asymmetric formations (J-like, and echelons) as well. To understand the role of anisotropy in the emergence of such patterns, we study how the configurations depend on the repulsion angle  $\alpha_r$ , while we keep fixed  $\alpha_c = 360^\circ$ .<sup>1</sup>

First, in Figure 6 where we plot the distribution of the angles between the nearest neighbor and the direction of motion (the horizontal axis), for four

<sup>1</sup>To obtain sharper evidence from simulations, it is useful to strengthen repulsion with respect to cohesion, taking a value of  $\xi$  larger than for lines: in the following simulations we set  $\xi = 13$ , and we also set  $n = 7$  and  $v_{\max} = 10$ .

values of  $\alpha_r$ . It is apparent that, if  $\alpha_r > 180^\circ$ , animals do not show any distinct preference. Instead, if  $\alpha_r < 180^\circ$ , animals show a distinct preference for keeping a specific angle, namely  $\frac{\alpha_r}{2}$ , with respect to their nearest neighbor.

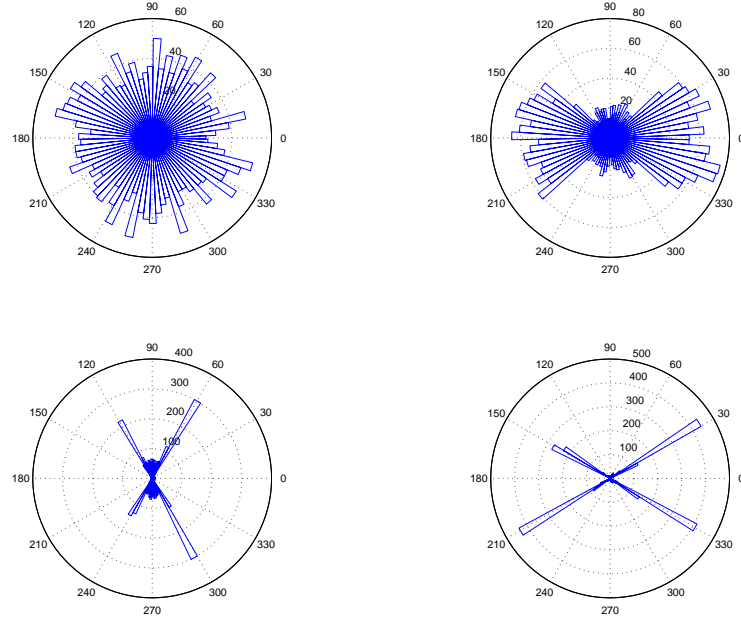


Figure 6: Distribution of the nearest–neighbor angle for  $\alpha_r = 360^\circ, 270^\circ, 120^\circ, 60^\circ$ . Data from 100 runs.

Second, to obtain more quantitative results about the transition from clusters to Vees, we introduce an Alignment Index (AI), defined as follows.  $AI(\theta)$  is the percentage of individuals whose nearest neighbor is positioned (up to a small tolerance  $\varepsilon_{\text{angle}}$ ) at a given angle  $\theta$  with respect to them. The dependence on  $\alpha_r$  of this novel index is shown in Figure 7. The figure plots both  $AI(\alpha_r/2)$  and  $AI(30^\circ)$ , computed as the average over 100 runs, with  $\varepsilon_{\text{angle}} = 3^\circ$ . If  $\alpha_r > 180^\circ$  the alignment index is as low as in a random configuration; if instead  $\alpha_r < 180^\circ$ , the high index confirms the preference for an  $\frac{\alpha_r}{2}$ -alignment. Qualitative analysis of the obtained configurations confirm these results: one observes that for a wide range of  $\alpha_r$ , a scenario sets up, in which the animals form (several) V-like formations. Examples are given in Figure 8. Finally, it can be noted from Figure 9 that the number of considered neighbors  $n$  affects the ability to form V-like configurations: if  $n$  is too small ( $n = 1$ ) or too large ( $n = N - 1$ ), the interesting patterns do not show up.

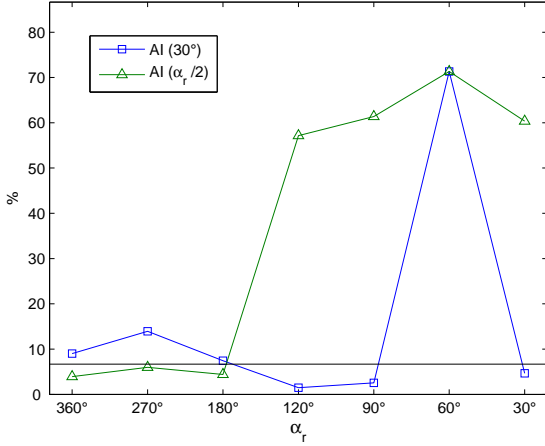


Figure 7:  $AI(30^\circ)$  and  $AI(\alpha_r/2)$  as functions of  $\alpha_r$ . Average of 100 runs. The reported reference value 6% is the expected value of AI from a random uniform distribution.

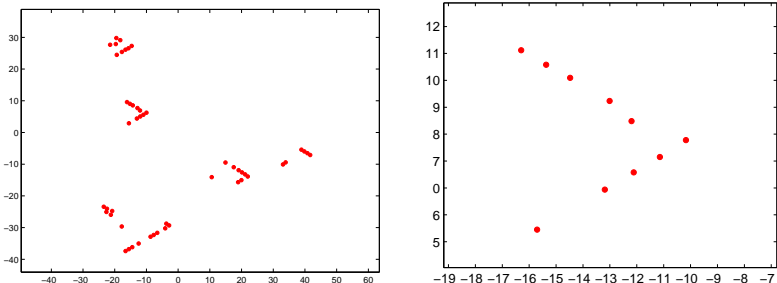


Figure 8: V-like formations obtained with  $\alpha_r = 60^\circ$ ,  $N = 30$ . The plot on the right is a close-up on one of the Vees.

## 4 Analytical results

In this section, which has a more technical mathematical content, we develop a framework for the analysis of the presented model, which helps the interpretation of the simulation results. Several analytical tools have been developed and used in the literature for the analysis of flocking algorithms. The typical method for their analysis consists in defining a suitable potential function, called “virtual” or “artificial” potential, whose gradient gives the dynamics. Hence a well developed theory on potential systems can be used to make a full mathematical analysis (see e.g. [30, 26]). We have anticipated in the introduction that our model has two main features: *state dependent switching*, and *asymmetry of interactions*. Let us illustrate them. It is clear from their definition that the sets

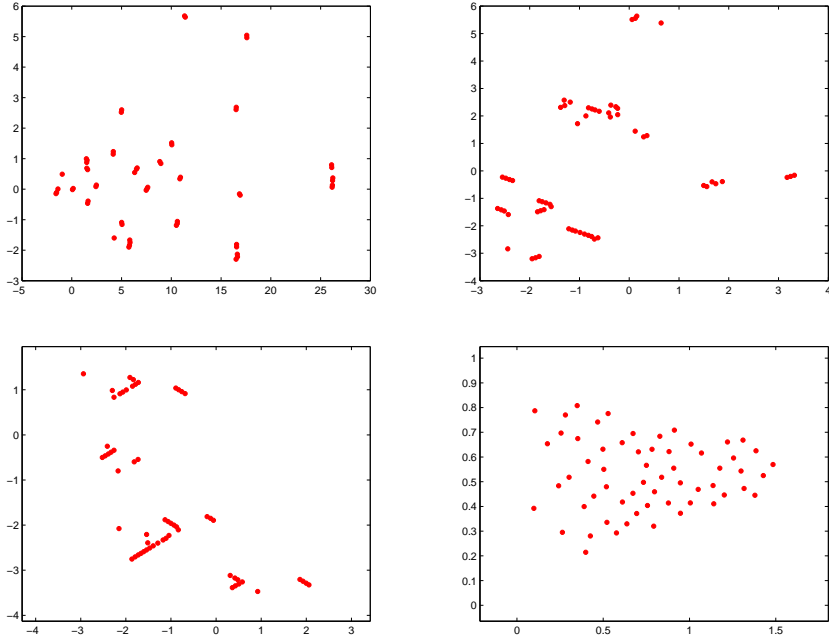


Figure 9: Configurations obtained with  $n = 1, 3, 7, N - 1$ , respectively, and  $\alpha_r = 60^\circ$ ,  $N = 60$ .

of cohesion and repulsion neighbors,  $\mathcal{C}^n$  and  $\mathcal{R}^n$ , depend on the configuration, that is on the state of the system, in a discontinuous way. As a consequence, depending on these sets, the system's evolution switches among a finite set of equations. Hence, from the system-theoretical point of view, equation (3) is a switching system with state dependent switches. These reasons make the analysis challenging, asking for the advanced system-theoretical tools developed for switching systems [13, 27, 2]. These issues have already been taken into account in flocking studies, as many papers consider the case of animals interacting when closer than a certain threshold: see, among others, [41]. Indeed, the virtual potentials approach can be extended to these problems, provided the potential is allowed to be non-smooth, that is not differentiable, at the switching points. However, our model has the distinctive feature that, because of the limitation in the number of neighbors and of the shape of the sensitivity zones, interactions need not be symmetric. Example giving, for two animals  $i, j$ , the inclusion  $j \in \mathcal{C}_i^n$  does not imply that  $i \in \mathcal{C}_j^n$ . This fact prevents us from using a virtual potentials approach, as the operation of differentiating the potential does not keep any directionality information. Actually, in the literature there is no general approach available for systems with directed interactions: a partial asymmetry has been taken into account in other works [37], but the given treatment is far for being sufficient for our purposes. In what follows we lay

down the basics of a theory that we believe is able to catch the specific features of our model.

Let us start by defining solutions of a switching system in an useful sense. Indeed, a differential equation of the form  $\dot{x} = f(x)$  with a discontinuous right-hand-side can not have a solution in the classical sense, i.e. a solution which is differentiable. Let us consider the right-hand side of equation (3). That expression is not defined on the set of *degenerate configurations*, that is

$$S = \{x \in (\mathbb{R}^2)^N \mid \exists i, j \in \{1, \dots, N\} \text{ s.t. } x_i = x_j\}.$$

Moreover, it is not always well defined on the set of *switching configurations*, in which two or more agents are equidistant from another,

$$D = \{x \in (\mathbb{R}^2)^N \mid \exists i, j, k \in \{1, \dots, N\} \text{ s.t. } \|x_i - x_j\| = \|x_i - x_k\|\},$$

because of the ambiguity in the definition of the “ $n$  closest neighbors”.

To have a proper definition, we shall consider the following differential equation

$$\dot{x}(t) = f(x(t)), \quad (4)$$

where the flow  $f : (\mathbb{R}^2)^N \setminus (D \cup S) \rightarrow (\mathbb{R}^2)^N$  is defined componentwise as in equation (3),

$$f_i(x) = \sum_{j \in \mathcal{C}_i^n} (x_j - x_i) - \xi^2 \sum_{j \in \mathcal{R}_i^n} \frac{(x_j - x_i)}{\|x_j - x_i\|^2} \quad \forall i \in \{1, \dots, N\}.$$

Note that  $f$  can not be extended with continuity to the set  $D \cup S$ . Hence, a solution involving, for instance, two animals equidistant from a third one, can not be even defined in the classical sense. In what follows, we shall extend the definition of the solutions of equation (4) to include the set  $D$ . For such extension, we shall follow the approach in [13], which requires defining a suitable *differential inclusion*, derived from (4).

To this goal, let  $B(y, \delta)$  denote the Euclidean ball of radius  $\delta$ , centered in  $y$ , and set

$$\mathcal{K}f(y) = \bigcap_{\delta > 0} \bigcap_{\mu(N)=0} \overline{\text{co}} \{f(B(y, \delta) \setminus N)\},$$

where the operator  $\overline{\text{co}}$  denotes closed convex hull, and  $\mu$  denotes Lebesgue measure. The map  $x : \mathbb{R}_{\geq 0} \rightarrow (\mathbb{R}^2)^N$  is said to be a *Filippov solution* of the system (4) if it is absolutely continuous and it satisfies the differential inclusion

$$\dot{x}(t) \in \mathcal{K}f(x(t))$$

for almost any  $t > 0$ .

From now on, we restrict ourselves to the case in which  $\alpha_c = 360^\circ$ ,  $\alpha_r = 360^\circ$ , and  $n = 1$ . Hence, each animal interacts just with its closest mate, and  $\mathcal{C}_i^1 = \mathcal{R}_i^1$  for every  $i$ . We make this assumption because, while the analysis for this case is simpler than for the general one, still the significant features of switching and

asymmetry are apparent. Indeed, provided  $N > 2$ , the relation of “being the closest to” needs not to be symmetrical. Moreover, simulations show for this case the formation of regular structures, as in Figure 3, which can be of interest in themselves.

Given the above definitions, we are able to state the following result.

**Proposition 4.1 (Existence)** *Equation (3) has at least one Filippov solution  $x(t)$ , for any initial condition  $x^0 \in (\mathbb{R}^2)^N \setminus S$ .*

*Proof:* We remark that  $f$  is piecewise continuous in the following sense. Let

$$\mathcal{V} = \{v \in \{1, \dots, N\}^N \mid \forall i \in \{1, \dots, N\}, v_i \neq i\}. \quad (5)$$

For any  $v \in \mathcal{V}$ , let us also define the open, possibly empty, set

$$E_v = \{x \in (\mathbb{R}^2)^N \setminus S \mid \forall i \in \{1, \dots, N\}, \|x_{v_i} - x_i\| < \|x_k - x_i\|, k \notin \{i, v_i\}\}$$

which is the set of the configurations such that  $v_i$  is  $i$ ’s closest neighbor. Note that  $E_v \cap E_u = \emptyset$  if  $u \neq v$ , the measure of the boundary of each  $E_v$  is zero, and, provided  $\bar{E}_v$  denotes the closure of  $E_v$  in the induced topology of  $(\mathbb{R}^2)^N \setminus S$ , it holds that  $\bigcup_{v \in \mathcal{V}} \bar{E}_v = (\mathbb{R}^2)^N \setminus S$ . In the interior of each “piece”  $E_v$ , that is if  $x \in E_v$ , we have that  $f(x) = f^v(x)$ , where the function  $f^v$  is defined componentwise as

$$f_i^v(x) = (x_{v_i} - x_i) - \xi^2 \frac{x_{v_i} - x_i}{\|x_{v_i} - x_i\|^2}.$$

Moreover, each function  $f^v$  is continuous in  $\bar{E}_v$ . Hence, we have that for every  $x$ , the set  $\mathcal{K}f(x)$  is nonempty, closed and convex, and the map  $x \mapsto \mathcal{K}f(x)$  is upper semicontinuous. This allows to apply [13, §7 Theorem 1], and obtain that the differential inclusion  $\dot{x}(t) \in \mathcal{K}f(x(t))$  has at least one solution  $x(t)$ , for any initial condition  $x^0 \in (\mathbb{R}^2)^N \setminus S$ . Equivalently, existence of solutions is guaranteed in the Filippov sense.  $\square$

**Remark 4.2** The above proof can be extended to the case  $n > 1$  and  $\alpha_c < 360^\circ$ ,  $\alpha_r < 360^\circ$ , modulo a suitable redefinition of the “pieces”  $E_v$ , in order to account for the more complex neighborhood relationships: the notational setup would be cumbersome, and we do not detail it.

Loosely speaking, we would expect that a configuration having the closest neighbor(s) at distance  $\xi$  for all animals, as in the lattice configuration of Figure 3 would be an equilibrium configuration. Indeed, each animal  $i$  is driven by the cohesion-repulsion force component  $f_i$  towards keeping a distance  $\xi$  from its neighbors. The following result technically clarifies this fact. Before the statement, we need a definition and a useful notation. First, we define a configuration  $x^*$  to be a *Filippov equilibrium* of  $f$  when  $0 \in \mathcal{K}f(x^*)$ . Second, we define the set of the closest neighbors of a given animal  $i \in \{1, \dots, N\}$  as

$$\text{closest}_i(x) = \arg \min_{j \neq i} \{\|x_i - x_j\|\}.$$

Notice that  $\text{closest}_i(x)$  may be multivalued, and let  $|\text{closest}_i(x)|$  denote its cardinality, that is the number of closest neighbors of animal  $i$ .

**Proposition 4.3 (Equilibria)** *Let  $x^* \in (\mathbb{R}^2)^N \setminus S$ . If for all  $i \in \{1, \dots, N\}$  and for all  $k \in \text{closest}_i(x^*)$ , it holds  $\|x_i^* - x_k^*\| = \xi$ , then  $x^*$  is a Filippov equilibrium for the system (3), and moreover  $1 \leq |\text{closest}_i(x^*)| \leq 6$ , for all  $i \in \{1, \dots, N\}$ .*

*Proof:* We shall now consider  $\text{closest}_i(x^*)$  for every  $i \in \{1, \dots, N\}$ , and distinguish the cases in which their cardinalities are equal to, or larger than 1. If  $|\text{closest}_i(x^*)| = 1$  for all  $i \in \{1, \dots, N\}$ , then  $f$  is smooth at  $x^*$ , and hence  $\mathcal{K}f(x^*) = \{f(x^*)\} = \{0\}$ . If instead there exists  $h \in \{1, \dots, N\}$  such that  $|\text{closest}_h(x^*)| > 1$ , then let us consider the set  $\mathcal{V}$  defined in (5), and take  $v \in \mathcal{V}$  such that  $v_i \in \text{closest}_i(x^*)$ , for every  $i \in \{1, \dots, N\}$ . Since  $x^*$  is an accumulation point of  $E_v$ , let us consider a sequence  $\{x^l\}_{l \in \mathbb{N}} \subset E_v$ , such that  $x^l \rightarrow x^*$  as  $l \rightarrow +\infty$ . Hence,  $f(x^l) \rightarrow 0$  as  $l \rightarrow \infty$ , and this implies, by the definition of the differential inclusion, that  $0 \in \mathcal{K}f(x^*)$ .

By definition,  $|\text{closest}_i(x^*)| \geq 1$ . The fact that  $|\text{closest}_i(x^*)| \leq 6$  can be shown by contradiction. Let  $|\text{closest}_i(x^*)| = m$ , with  $m > 6$ , for some  $i$ . Then there are  $m$  points of  $\mathbb{R}^2$ , representing positions, which have to belong to a circle of radius  $\xi$  centered in  $x_i^*$ . But then the distance of at least two of them has to be less than  $\xi$ , which is a contradiction.  $\square$

Hexagonal lattice configurations, in which animals are at distance  $\xi$  from their closest neighbor(s), have been observed in simulations (Figure 3) in the case  $\alpha_c = 360^\circ$ ,  $\alpha_r = 360^\circ$ , and  $n = 1$ . Indeed, Proposition 4.3 shows that such a lattice is an equilibrium: loosely speaking, we can say that it is the most closely packed configuration among the equilibria pointed out by this result. Notice moreover that such lattice equilibria are actually switching configurations, belonging to the set  $D$ : this gives an a posteriori justification of the effort that we have done for a careful extension of the solutions to this set.

## 5 Discussion

Our agent-based model has been conceived from assumptions which are widely accepted from the biological point of view, and it shows the onset of group structures and patterns which are observed in nature. In some sense, our model can be seen as a generalization of other similar models, since in the special case  $(\alpha_r, \alpha_c) = (360^\circ, 360^\circ)$  we recover results which are by now consolidated in the literature. The novelty resides in that by modifying a small set of key parameters, we obtain other patterns, which are experimentally observed in animal groups (for example, lines by lobsters [5], elephants and penguins, V-like formations by geese). Our results suggest that apparently large differences in group patterns could arise just from differences in the cohesion and repulsion sensitivity zones, namely in the ranges of distance and angles in which they are active. In this perspective, we would like to point out that the group structure is

not only a function of the species, but also of the environment and individuals conditions. For instance, surf scoters [28] and other animals can form either clusters or lines, depending on the environment conditions. This suggests that  $\alpha_r$  and  $\alpha_c$  are not only animal-dependent, but they can also vary depending on the type of motion, environmental condition, presence of predators, and aim of the displacement. In this paper, the choices of the angles were made to explore the model's properties and they do not come from experimental data. Nevertheless, the correspondence of the simulated patters with those experimentally observed suggests that future research should distinguish, in modeling interactions, between the (variable) sensitivity zones and the (fixed) visual field, as in [17, 31], and should also investigate this distinction in real animals.

Now we review the results obtained in the previous sections, trying to propose some biological insights, especially regarding the role of anisotropy in the interactions. As we did presenting the simulations, we distinguish three cases: isotropic cohesion and repulsion; anisotropic cohesion and repulsion; isotropic cohesion and anisotropic repulsion.

In the first case, with completely isotropic interactions, our model produces clusters of individuals. Clusters are common for small birds (e.g., starlings [4]) and for fish, whose sensing abilities allow an almost complete perception around them. Moreover, these animals often change the direction of motion following complex trajectories, and this makes useful to keep under control all the space around. By means of isotropic interactions, they are able to change rapidly the direction of motion of the whole group, with no need to re-arrange significantly the shape of the group in function of the new direction: this would not be possible in less symmetric formations like lines or Vees.

Instead, when interactions are not isotropic, also the obtained formations are not isotropic, and we observe that their onset depends on spontaneous leader-following mechanisms. When both repulsion and cohesion are focused in front, following the direction of motion, an evident leader-following mechanism sets up, which induces the formation of lines. Lines are commonly observed in slow-moving animals as lobsters [5], elephants and penguins. The small repulsion angle  $\alpha_r$  appears to be crucial to obtain such a pattern (see Figure 4): this could be related to the fact that such animals keep a steady direction of motion, and, once the line is established, repulsion needs to be active only against the forerunners. The choice  $\alpha_c = 180^\circ$  is also very significant from the biological point of view. Indeed, this means that individuals pay more attention to the group mates in front, while they do not respond to what happens behind them. For example, they would not perceive a disconnection of the group. Hence, a model assuming  $\alpha_c = 180^\circ$  seems suitable for “selfish” animals which find advantageous to follow the head of the group, where informed individuals are, but do not aim at the cohesion of the whole group.

A different leader-following mechanism induces V-like formations, coming from the fact that cohesion is isotropic, and repulsion is restricted to the group mates in front. Our simulations reproduce several significant features of natural

V-like formations, described in the experimental literature [15, 21, 18]. First, echelons and Jays are as common as perfect Vees: in our model a perfect Vee is not preferable to Jays and echelons, and actually the individual's behavior does not depend on the global shape of the formation. Second, V-like formations are not stable, but rather they often disband and quickly reform. Third, each Vee is made of few individuals (about 5 for echelons and 10 for Vees in the majority of cases), independently of the total number of animals  $N$ . In other words, increasing  $N$  leads to the formation of a larger number of V-like groups, but not to larger ones. This fact, observed in the field [18], can be explained [35] resorting to the argument of string instability (see Section 3.2): large V-like groups are rarely observed in nature because they are not stable. Our results should be compared to those in [31], where the authors propose an ad-hoc formation algorithm, motivated by aerodynamic issues. In that paper the number of V-like groups is constant for increasing  $N$ .

V-like formation has been greatly investigated (see for instance [18, 12, 38, 45, 35] and references therein), but its function is not completely understood yet. Two hypothesis are the most considered: aerodynamic advantage, and visual communication advantage. The former is based on the fact that each flying individual creates an upwash region behind it, just off the tips of its wings, such that another individual can benefit placing itself in that region. The latter is instead based on the fact that flying in a skewed position relative to the bird in front helps to avoid collisions, and at the same time allows an unhindered visual communication with all the group mates [12]. Our results support the hypothesis of visual communication advantage (although without negating the reasons of the aerodynamic one), since V-like formations are not obtained imposing that individuals place themselves in the upwash region of a group mate, as in [31]. Instead, we simply assume a restricted repulsion angle, which avoids to have a group mate too close in front, and isotropic cohesion force, for the sake of group cohesion. In opposition to lines, here the large-range cohesion could be associated to the fact that each individual has an interest in waiting for the followers, and that *all* the group reaches the final target.

Besides investigating the role of anisotropy of interaction, we have also investigated the dependence of the configurations on  $n$ , the number of interacting neighbors. At least two remarks are in order. First, cluster configurations can be obtained with any  $n$ , but the chosen value of  $n$  influences the internal structure of the cluster. Second, to obtain lines or V-like formations an intermediate number of neighbors, about  $n = 7$ , is preferable. This result relates to experimental evidence indicating that birds take into account seven neighbors during flight [3]. To conclude, our results confirm that it is reasonable to assume topological interactions with a limited number of neighbors.

## Future research

Besides investigating the biological significance of the presented model, in the next future we want to develop our research in three aspects. First, we have

noticed that although the presented model is bidimensional, it can readily be extended to a three-dimensional one. As 3D collective motion is a topic of relevant interest, we are planning to develop a 3D version of our model: the novel set of simulations might show interesting phenomena. Indeed, in three dimensions much richer dynamics are possible: we are especially interested in studying the effect of the anisotropy in 3D V-like formations, as skewed formations as described in [21] are inherently three-dimensional.

Second, we want to further develop the theoretical analysis of the model, in order to include a wider description of the equilibria of (2), and their stability analysis. As we said, several models similar to ours have been investigated in the literature – see for instance the thorough analysis of the potential laws in [30]. However, we believe that anisotropic and topological interactions can be better understood by the switching systems approach that we took in Section 4, taking advantage of the theoretical instruments developed in mathematics [13] and widely used in engineering [27], also in relation with flocking problems [41]. Moreover, we would be interested in a variational interpretation of the model. Indeed, while it is apparent that each animal is trying to minimize a “private” potential depending on its neighbors, it is unclear whether and when this would result in a configuration minimizing some global objective function. This kind of remarks relates our problem to more general problems of distributed optimization [33, 34], in which groups of agents collaborate in order to optimize an objective function, which they may not completely know. We believe that the application of these mathematical tools to biological models can provide novel insights for their understanding, and enrich the set of tools available to the mathematical biology community.

Third, we are confident in the engineering applications of the proposed biologically-inspired switching system. In our opinion, a deeper analysis of the model is not only of interest in itself, but also preliminary to the application of these ideas to the design of robust algorithms for formation cruising of unmanned vehicles. The latter problem is one of the challenges of contemporary engineering, and has been studied in many works: among them, we recall [41, 6]. We believe that the simplicity of the interaction rules we have proposed, and the limited number of group mates to be kept into account for their application, can be interesting features for engineering applications.

## References

- [1] I. Aoki. An analysis of the schooling behavior of fish: internal organization and communication process. *Bull. Ocean Res. Inst. Univ. Tokyo*, 12:1–65, 1980.
- [2] A. Bacciotti. Stabilization by means of state space depending switching rules. *Systems & Control Letters*, 53:195–201, 2004.
- [3] M. Ballerini, N. Cabibbo, R. Candelier, A. Cavagna, E. Cisbani, I. Giardina, V. Lecomte, A. Orlandi, G. Parisi, A. Procaccini, M. Viale, and

V. Zdravkovic. Interaction ruling animal collective behavior depends on topological rather than metric distance: Evidence from a field study. *Proceedings of the National Academy of Sciences of the United States of America*, 105(4):1232–1237, 2008.

- [4] M. Ballerini, N. Cabibbo, R. Candelier, A. Cavagna, E. Cisbani, I. Giardina, A. Orlandi, G. Parisi, A. Procaccini, M. Viale, and V. Zdravkovic. Empirical investigation of starling flocks: a benchmark study in collective animal behaviour. *Animal Behaviour*, 76:201–215, July 2008.
- [5] R. G. Bill and W. F. Herrnkind. Drag reduction by formation movement in spiny lobsters. *Science*, 193(4258):1146–1148, 1976.
- [6] F. Bullo, J. Cortés, and S. Martínez. *Distributed Control of Robotic Networks*. Applied Mathematics Series. Princeton University Press, 2009.
- [7] D. Chao and S. A. Levin. A simulation of herding behavior: The emergence of large-scale phenomena from local interactions. In S. Ruan, G.S.K. Wolkowicz, and J. Wu, editors, *Differential Equations with Applications to Biology*, volume 21 of *Fields Institute Communications*, pages 81–95. AMS, Providence, RI, 1999.
- [8] Y. Chuang, M. R. D’Orsogna, D. Marthaler, A. L. Bertozzi, and L. S. Chayes. State transitions and the continuum limit for a 2D interacting, self-propelled particle system. *Physica D*, 232(1):33–47, 2007.
- [9] I. D. Couzin, J. Krause, N. R. Franks, and S. A. Levin. Effective leadership and decision-making in animal groups on the move. *Nature*, 433(7025):513–516, 2005.
- [10] I. D. Couzin, J. Krause, R. James, G. D. Ruxton, and N. R. Franks. Collective memory and spatial sorting in animal groups. *Journal of Theoretical Biology*, 218:1–11, 2002.
- [11] F. Cucker and S. Smale. Emergent behavior in flocks. *IEEE Transactions on Automatic Control*, 52(5):852–862, 2007.
- [12] C. Cutts and J. Speakman. Energy savings in formation flight of pink-footed geese. *Journal of Experimental Biology*, 189:251–261, 1994.
- [13] A. F. Filippov. *Differential Equations with Discontinuous Righthand Sides*, volume 18 of *Mathematics and Its Applications*. Kluwer Academic Publishers, 1988.
- [14] I. Giardina. Collective behavior in animal groups: theoretical models and empirical studies. *HFSP Journal*, 2(4):205–219, 2008.
- [15] L. L. Gould and F. H. Heppner. The vee formation of canada geese. *Auk*, 91:494–506, 1974.

- [16] G. Grégoire, H. Chaté, and Y. Tu. Moving and staying together without a leader. *Physica D*, 181(3-4):157–170, 2003.
- [17] S. Gueron, S. A. Levin, and D. I. Rubenstein. The dynamics of herds: from individuals to aggregations. *Journal of Theoretical Biology*, 182:85–98, 1996.
- [18] F. R. Hainsworth. Precision and dynamics of positioning by canada geese flying in formation. *Journal of Experimental Biology*, 128:445–462, 1987.
- [19] W. D. Hamilton. Geometry for the selfish herd. *Journal of Theoretical Biology*, 31:295–311, 1971.
- [20] C. K. Hemelrijk and H. Hildenbrandt. Self-organized shape and frontal density of fish schools. *Ethology*, 114(3):245–254, 2008.
- [21] F. H. Heppner. Avian flight formations. *Bird-Banding*, 45:160–169, 1974.
- [22] A. Huth and C. Wissel. The simulation of the movement of fish schools. *Journal of Theoretical Biology*, 156(3):365–385, 1992.
- [23] Y. Inada and K. Kawachi. Order and flexibility in the motion of fish schools. *Journal of Theoretical Biology*, 214(3):371–387, 2002.
- [24] J. Krause and G. D. Ruxton. *Living in groups*. Oxford Series in Ecology and Evolution. Oxford, 2002.
- [25] H. Kunz and C. K. Hemelrijk. Artificial fish schools: collective effects of school size, body size, and body form. *Artificial Life*, 9(3):237–253, 2003.
- [26] Y. X. Li, R. Lukeman, and L. Edelstein-Keshet. Minimal mechanisms for school formations in self-propelled particles. *Physica D*, 237(5):699–720, 2008.
- [27] D. Liberzon. *Switching in systems and control*. Springer, 2003.
- [28] R. Lukeman and L. Edelstein-Keshet. Personal communication, 2009.
- [29] R. Lukeman, Y.-X. Li, and L. Edelstein-Keshet. A conceptual model for milling formations in biological aggregates. *Bulletin of mathematical biology*, 71(2):352–382, 2009.
- [30] A. Mogilner, L. Edelstein-Keshet, L. Bent, and A. Spiros. Mutual interactions, potentials, and individual distance in a social aggregation. *Journal of Mathematical Biology*, 47(4):353–389, 2003.
- [31] A. Nathan and V. C. Barbosa. V-like formations in flocks of artificial birds. *Artificial Life*, 14:179–188, 2008.
- [32] J. K. Parrish, S. V. Viscido, and D. Grunbaum. Self-organized fish schools: An examination of emergent properties. *Biological Bulletin*, 202(3):296–305, 2002.

- [33] M. Rabbat and R. Nowak. Distributed optimization in sensor networks. In *Symposium on Information Processing of Sensor Networks (IPSN)*, pages 20–27, Berkeley, USA, April 2004.
- [34] R. L. Raffard, C. J. Tomlin, and S. P. Boyd. Distributed optimization for cooperative agents: Application to formation flight. In *IEEE Conf. on Decision and Control*, pages 2453–2459, December 2004.
- [35] P. Seiler, A. Pant, and J. K. Hedrick. A systems interpretation for observations of bird v-formations. *Journal of Theoretical Biology*, 221(2):279–87, 2003.
- [36] P. Seiler, A. Pant, and K. Hedrick. Disturbance propagation in vehicle strings. *IEEE Transactions on Automatic Control*, 49(10):1835–1842, 2004.
- [37] H. Shi, L. Wang, and T. Chu. Virtual leader approach to coordinated control of multiple mobile agents with asymmetric interactions. *Physica D*, 213:51–65, 2006.
- [38] J. R. Speakman and D. Banks. The function of flight formations in Greylag Geese *Anser anser*; energy saving or orientation? *Ibis*, 140:280–287, 1998.
- [39] D. J. T. Sumpter. The principles of collective animal behaviour. *Phil. Trans. R. Soc. B*, 361:5–22, 2006.
- [40] D. Swaroop and J. K. Hedrick. String stability of interconnected systems. *IEEE Transactions on Automatic Control*, 41(3):349–357, 1996.
- [41] H. G. Tanner, A. Jadbabaie, and G. J. Pappas. Flocking in fixed and switching networks. *IEEE Transactions on Automatic Control*, 52(5):863–868, 2007.
- [42] J. H. Tien, S. A. Levin, and D. I. Rubenstein. Dynamics of fish shoals: identifying key decision rules. *Evolutionary Ecology Research*, 6:555–565, 2004.
- [43] T. Vicsek, A. Czirók, E. Ben-Jacob, I. Cohen, and O. Shochet. Novel type of phase transition in a system of self-driven particles. *Physical Review Letters*, 75(6):1226–1229, 1995.
- [44] K. Warburton and J. Lazarus. Tendency-distance models of social cohesion in animal groups. *Journal of Theoretical Biology*, 150:473–488, 1991.
- [45] H. Weimerskirch, J. Martin, Y. Clerquin, P. Alexandre, and S. Jiraskova. Energy saving in flight formation. *Nature*, 413:697–698, 2001.